Organometallic complexes for second-order non-linear optics: synthesis and molecular quadratic hyperpolarizabilities of η^5-monocyclopentadienyliron(II) nitrile derivatives with different phosphines. X-ray crystal structure of [FeCp(DPPE)(p-NCC$_6$H$_4$NO$_2$)][PF$_6$]·CH$_2$Cl$_2$

M. Helena Garcia [a,b,*], M. Paula Robalo [a,c], A.R. Dias [a], M. Fátima M. Piedade [a,b], Adelino Galvão [a], Wim Wenseleers [d], Etienne Goovaerts [d]

[a] *Centro de Química Estrutural, Instituto Superior Técnico, Av. Rovisco Pais, 1049-001 Lisbon, Portugal*
[b] *Departamento de Química e Bioquímica, Faculdade de Ciências da Universidade de Lisboa, Campo Grande, 1749-016 Lisbon, Portugal*
[c] *Departamento de Química, Universidade de Évora, Colégio Luís António Verney, Rua Romão Ramalho n° 59, 7000-671 Évora, Portugal*
[d] *Physics Department, University of Antwerp (UIA), Universiteitsplein 1, 2610 Wilrijk, Antwerp, Belgium*

Abstract

New complexes of the type [FeCp(P_P)(p-NCR)][PF$_6$] (P_P = (S)-PROLOPHOS, DPPE and (R)-PROPHOS ((S)-PRO-LOPHOS = (S)-N-(diphenylphosphino)-2-diphenylphosphinooxymethylpyrrolidine; DPPE = 1,2-bis(diphenylphosphino)ethane; (R)-PROPHOS = (R)-(+)-1,2-bis(diphenylphosphino)propane); R = C$_6$H$_4$N(CH$_3$)$_2$, C$_6$H$_4$NO$_2$, (E)-C(H)=C(H)C$_6$H$_4$NO$_2$, C$_6$H$_4$C$_6$H$_4$NO$_2$) have been synthesized and characterized. Spectroscopic data were evaluated in order to correlate the tuning of the electronic density at the metal center with the first molecular hyperpolarizabilities (β) determined by hyper-Rayleigh scattering at 1064 nm. Experimental β values increase with chain length and with the enhancement of the donor ability of the bidentate phosphine. [FeCp(DPPE)((E)-p-NC–C(H)=C(H)C$_6$H$_4$NO$_2$)][PF$_6$] is found to have the highest β value (570×10^{-30} esu) in the series. Molecular orbital calculations were carried out to understand the geometric and electronic factors involved and also to compute the static hyperpolarizabilities, β_0. These results are consistent with the trend observed in the β_0 values derived from experiment on the basis of the two-level model. The complex [FeCp(DPPE)(p-NCC$_6$H$_4$NO$_2$)][PF$_6$] was crystallographically characterized. The compound crystallizes in the centrosymmetric space group *Pbcn*. Bond distances within the nitrile ligand were discussed in order to evaluate the extension of π-backdonation suggested by spectroscopic data. © 2001 Elsevier Science B.V. All rights reserved.

1. Introduction

The development of novel materials for non-linear optical (NLO) applications has been a very active area of research for a number of years [1–4]. Although a great deal of work has been carried out on the investigation of the non-linear optical properties in inorganic materials and organic molecules, the optical non-linearities of organometallic complexes has started to be actively studied more recently [5].

The general criteria for obtaining organic molecules with large first hyperpolarizability (β) are being applied in the search for molecular organometallic NLO materials. Accordingly, the basic strategy of using electron-donor and electron-acceptor substituents to polarize the π-electron system of organic molecules, thereby creating the possibility of a second-order non-linear optical response, has been extended to organometallic compounds consisting of conjugated donor–acceptor systems [1–5].

* Corresponding author.
E-mail address: i017@alfa.ist.utl.pt (M.H. Garcia).

Our earlier studies in this field [6] reported for $[FeCp((+)-DIOP)(p-NCC_6H_4NO_2)][PF_6]$ ((+)-DIOP = (+)-2,3-O-isopropylidene-2,3-dihidroxy-1,4-bis-(diphenylphosphino)butane) a SHG efficiency of 38 times the urea standard, measured by Kurtz powder technique. Spectroscopic evidence was found to support the idea that the $[FeCp((+)-DIOP)]^+$ fragment was acting as a π-donor via d-π*(NC) orbitals towards the NO_2 acceptor group, enhancing the molecular first hyperpolarizability (β) of the coordinated nitrile, which was related to the increased non-linear optical properties. Further studies on ruthenium(II) analogs also yielded significant SHG results [7,8].

X-ray diffraction structures of some members of the families [9] showed the metal to be in the same plane as the π-system of the chromophore, which is responsible for the availability of d orbitals for π-delocalization towards the organic conjugated ligand. These results are in good agreement with results published before [10], suggesting the use of this structural feature as a design criterion to maximize the organometallic non-linear response.

Our further studies on a systematic series of metal fragments $(\eta^5-C_5H_5)M(P\_P)$ (M = Co(III), Ni(II), Ru(II) and Fe(II); P_P = phosphine ligand) with *para*-substituted benzonitrile ligands, by hyper-Rayleigh scattering (HRS) at the fundamental wavelength of 1064 nm, showed also that the iron(II) fragment is the most promising organometallic electron donor group [11].

These encouraging NLO results prompted us to extend our work on the η^5-monocyclopentadienyliron(II) system and to study the possibility of tuning the electron density at the metal center, through phosphine coligands. We report herein the synthesis of $[FeCp(P\_P)(p\text{-}NCR)]^+$ complexes with various bidentate phosphines, P_P = (S)-PROLOPHOS, DPPE and (R)-PROPHOS ((S)-PROLOPHOS = (S)-N-(diphenylphosphino)-2-diphenylphosphinooxymethylpyrrolidine; DPPE = 1,2-bis(diphenylphosphino)ethane; (R)-PROPHOS = (R)-(+)-1,2-bis(diphenylphosphino)propane), with different donor abilities. Also a single crystal X-ray study of $[FeCp(DPPE)(p\text{-}NCC_6H_4NO_2)][PF_6]$ is presented and discussed. The use of the chiral (R)-

PROPHOS phosphine, was considered as a good alternative to (+)-DIOP, since it is less bulky and therefore more appropriate for future studies of the NLO effect in the solid state.

Spectroscopic data were evaluated in order to understand the contribution of these coligands on the donor–acceptor ability of the iron(II) fragment and the degree of π-delocalization on the molecule as well. Measurements of the molecular quadratic hyperpolarizabilities for some of these compounds were carried out by HRS at the fundamental wavelength of 1064 nm in liquid solution. Extended Hückel MO calculations were carried out in two model compounds in order to understand the geometric and electronic factors that may be conditioning the design of new compounds showing large hyperpolarizabilities and ab initio calculations were performed to compute values of β_0 for these two model compounds.

Experimental β values were correlated with spectroscopic data in order to understand the molecular structure–NLO property relationship in view of a future optimization of the macroscopic NLO properties of this family of compounds.

2. Results and discussion

2.1. Preparation of the complexes $[FeCp(P\_P)(p\text{-}NCR)][PF_6]$

Nitrile complexes with different phosphines were prepared by iodide abstraction from the starting materials $[FeCp(P\_P)(I)]$ (P_P = (S)-PROLOPHOS, (R)-PROPHOS, DPPE (Fig. 1)) by $TlPF_6$ in the presence of a slight excess of nitrile, in dichloromethane at room temperature, following the procedure published before [6].

After workup, orange or red crystals of $[FeCp(P\_P)(p\text{-}NCR)][PF_6]$ (P_P = (S)-PROLOPHOS, R = $C_6H_4N(CH_3)_2$ (**1**), R = $C_6H_4NO_2$ (**2**); P_P = DPPE, R = $C_6H_4N(CH_3)_2$ (**3**), R = $C_6H_4NO_2$ (**4**), R = (E)-C(H)=C(H)$C_6H_4NO_2$ (**5**), R = $C_6H_4C_6H_4NO_2$ (**6**); P_P = (R)-PROPHOS, R = $C_6H_4N(CH_3)_2$ (**7**), R = C_6H_4-NO_2 (**8**)) were obtained in ca. 52–96% yield.
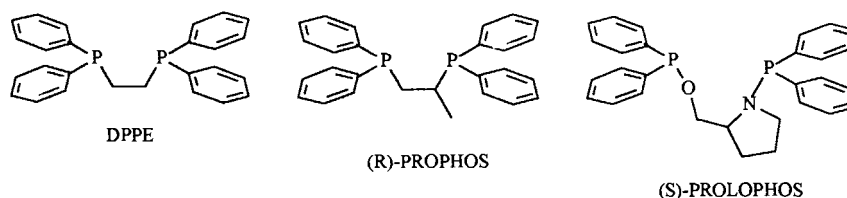

Fig. 1. Structural formulae of phosphines DPPE, (R)-PROPHOS and (S)-PROLOPHOS.

The compounds are fairly stable towards oxidation in air and to moisture both in the solid state and in solution. The formulation is supported by analytical data, IR and ^{1}H, ^{13}C and ^{31}P-NMR spectra (see Section 4). The molar conductivities of ca. 10^{-3} M solutions of the complexes in nitromethane, in the range 70–86 Ω^{-1} cm^2 mol^{-1}, are consistent with values reported for 1:1 electrolytes [12].

Typical IR bands confirm the presence of the cyclopentadienyl ligand (ca. 3060 cm^{-1}), the PF$_6^-$ anion (840 and 560 cm^{-1}) and the coordinated nitrile (ν(CN) at ca. 2200 cm^{-1}) in all complexes. No significant change was observed on ν(CN) upon coordination of the dimethylamino derivatives but in the case of *p*-NCC$_6$H$_4$NO$_2$, depending on the coordinated phosphine coligand, a significant negative shift was found, up to 35 cm^{-1} for the DPPE derivative. As we described before, this effect would result from enhanced π-backdonation owing to π-bonding between the metal d orbitals and the π^* orbital of the CN group [6].

Chemical shifts for the cyclopentadienyl ring are in the range usually observed for monocationic iron(II) complexes and seem to be affected both by the phosphine and by the nature of the coordinated nitrile. In fact, substitution of (*S*)-PROLOPHOS by the more electron donating phosphines (*R*)-PROPHOS or DPPE, has the expected effect on Cp resonances (a shift downfield of 0.26 and 0.36 ppm respectively, in the ^{1}H-NMR spectra) consistent with the increased Cp ring currents owing to the increased electron density at the metal center. Replacement of the donor group *p*-(N(CH$_3$)$_2$) by the acceptor group (*p*-NO$_2$) on the nitrile benzene ring gives a deshielding effect on the Cp resonance, as was observed previously for the analogous (+)-DIOP complexes [6]. The presence of different phosphine coligands is also confirmed by the signals of the carbon backbone in the corresponding ranges of the spectra. Conversely to the effect observed for Cp ring, the phosphine signals were relatively insensitive to the nature of the aromatic nitrile.

The effect on coordination of the nitriles to the different iron(II) fragments is mainly found in the shielding observed at the *ortho* (relative to the NC group) protons of the benzene ring. This shielding was found to vary from 0.05 ppm for [FeCp(*S*)-PROLOPHOS)(*p*-NCC$_6$H$_4$N(CH$_3$)$_2$)][PF$_6$] up to 1.16 ppm for [FeCp(DPPE)(*p*-NCC$_6$H$_4$NO$_2$)][PF$_6$]. Although in some cases this effect might be insignificant, a trend is clearly observed. The highest shielding on *ortho* protons was observed for the *p*-nitrobenzonitrile DPPE derivative, in which this effect is concomitantly combined with a deshielding on protons of the Cp ring, indicating clearly an electronic flow towards the aromatic protons due to a π-backdonation effect involving the metal center. These observed shifts are consistent with the possibility of some contribution of a vinylidene form in solution:

$$[Fe]^+-N{\equiv}C-C_6H_4-R \leftrightarrow [Fe]^{2+}=N=C=C_6H_4=R^-$$
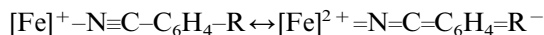
Comparison of these spectral data with our results on (+)-DIOP analogs [6] indicates that different phosphine coligands can tune the donor character of the organometallic fragment, in the following trend:

$$(S)\text{-PROLOPHOS} < (+)\text{-DIOP} < (R)\text{-PROPHOS}$$

$$\approx DPPE$$
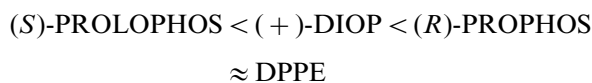
^{13}C-NMR data of this family of compounds confirm the evidence found for proton spectra. The Cp ring seems to be sensitive both to the coordinated nitrile and phosphine, being more shielded with the enhancement of donor ability of the phosphine. For the same phosphine a deshielding is observed when the N(CH$_3$)$_2$ donor group is replaced by the NO$_2$ acceptor group.

^{31}P-NMR data of complexes reported in ppm downfield from the external standard (85% H$_3$PO$_4$) showed the expected deshielding upon coordination of the phosphines. Accordingly this effect was enhanced with the better donor character of the phosphine, suggesting an easier release of electron density towards the metal center.
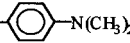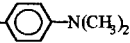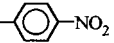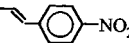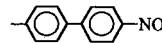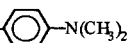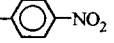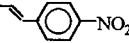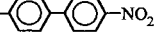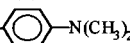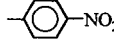
2.2. Electronic spectra

Optical absorption spectra of complexes [FeCp(P_P)(*p*-NCR)][PF$_6$] were recorded in ca. 1.5×10^{-4} M in dichloromethane, in the range of wavelengths 230–1100 nm (Table 1). In order to study the solvatochromic behavior for compound [FeCp(DPPE)((*E*)-*p*-NCC(H)=C(H)C$_6$H$_4$NO$_2$)][PF$_6$], the spectra were obtained in other solvents of increasing polarity (acetone and DMSO) in the same range of wavelengths (Fig. 3). The absorption spectra for all compounds are characterized by one intense absorption band in the UV region, attributed to electronic transitions occurring in the aromatic ligands. In addition, the nitro derivatives also present one extra broad band in the visible region characterized as a metal to ligand charge transfer (MLCT) band, since a comparable absorption maximum is not found either for the [FeCp(P_P)(I)] or for the uncoordinated nitrile precursors. In Fig. 2 spectra recorded for the compounds [FeCp(DPPE)(*p*-NCC$_6$H$_4$R)][PF$_6$] (R = N(CH$_3$)$_2$ and NO$_2$) typify the electronic spectra of this family of compounds, obtained in dichloromethane solution.

Chromophore chain lengthening leads to a slight bathochromic shift on $\lambda_{max.}$ (MLCT band), with [FeCp(P_P)(*p*-NCC(H)=C(H)C$_6$H$_4$NO$_2$)][PF$_6$] (P_P = (+)-DIOP, DPPE) complexes containing the lowest energy transitions, indicating that conjugation is slightly increased. Nevertheless in the case of biphenyl compounds, a hipsochromic shift of the low-energy absorption band was observed, suggesting a breaking of the conjugation through the second ring.

Table 1
Optical spectral data for complexes [FeCp(P_P)(p-NCR)][PF$_6$] in dichloromethane solutions at room temperature, concentration ca. 1.5×10^{-4} mol dm^{-3}

Compound [FeCp(P__P)(p-NCR)][PF$_6$]	λ_{exp} (nm)	$\varepsilon \times 10^4$ (M^{-1}cm^{-1})
P__P = (S)-PROLOPHOS		
R= —C$_6$H$_4$—N(CH$_3$)$_2$	296	6.38
	339	7.10
P__P = (+)DIOP		
R= —C$_6$H$_4$—N(CH$_3$)$_2$	295	0.90
	344	1.14
—C$_6$H$_4$—NO$_2$	255	3.01
	453	0.57
—CH=CH—C$_6$H$_4$—NO$_2$	288	3.67
	461	0.89
—C$_6$H$_4$—C$_6$H$_4$—NO$_2$	288	2.80
	387	0.76
P__P = DPPE		
R= —C$_6$H$_4$—N(CH$_3$)$_2$	296 (sh)	
	335	7.79
—C$_6$H$_4$—NO$_2$	251	3.05
	430	0.55
—CH=CH—C$_6$H$_4$—NO$_2$	293	2.03
	463	0.58
—C$_6$H$_4$—C$_6$H$_4$—NO$_2$	285	2.47
	372	0.83
	430 (sh)	
P__P = (R)-PROPHOS		
R= —C$_6$H$_4$—N(CH$_3$)$_2$	295	1.78
	334	2.20
—C$_6$H$_4$—NO$_2$	247	4.43
	447	0.73

The solvatochromic response of [FeCp(DPPE)(p-NCC(H)=C(H)C$_6$H$_4$NO$_2$)][PF$_6$] was studied and the results are shown in Fig. 3. A pronounced red shift in the position of the MLCT absorption band occurs when the solvent polarity is increased, with differences of ca. 40 nm, while the positions of the other bands remain almost unchanged. The positive solvatochromic behavior exhibited by the compound is characteristic of MLCT transitions with an increase of the dipole moment upon photoexcitation.

2.3. Second-order NLO characterization

The molecular second-order polarizabilities β of three DPPE complexes as well as their (+)-DIOP analogs were determined by means of hyper-Rayleigh scattering (HRS) in liquid solution [13,14] at a fundamental wavelength of 1064 nm. The HRS technique was chosen because it yields molecular hyperpolarizabilities that are much easier to interpret in terms of molecular structure–property relationships than Kurtz-powder results, since the latter also depend very strongly on bulk properties such as crystal packing, grain size and phase-matching effects. The more traditional electric field induced second harmonic generation (EFISHG) technique, in which a static electric field is applied to break the macroscopic centrosymmetry of the liquid and induce coherent frequency doubling, is not applicable to the studied ionic compounds. Instead, the HRS technique relies on the incoherent scattering of second harmonic light which results from the microscopic disorder (random orientation) of molecules in a liquid solution [15]. Molecular β values are deduced from the intensity of this second harmonic light as detailed in Section 4.4.

The experimental hyperpolarizabilities are shown in Table 2 for six of the Fe(II) complexes with the acceptor group NO$_2$, as well as for two of the ligands. Static polarizabilities are also listed as estimated from the two-level model using the lowest energy electronic transition corresponding to the long wavelength absorption band at λ_{eg}. This procedure has to be considered with caution, taking into account that near-resonance conditions occur for several of the compounds. As in the case of the ruthenium compounds, the hyperpolarizabilities (both β and β_0) of the complexes are much higher (one to two orders of magnitude) compared to the conjugated ligands. Starting from the shortest ligand (R = C$_6$H$_4$NO$_2$), a strong increase of β is observed when the conjugated chain length is increased by inserting a vinylene unit, for both the DPPE and (+)-DIOP derivatives. This is in good agreement with the spectroscopic data (e.g. red shift of the electronic transition) and confirms the idea that the high hyperpolarizabilities result from the extension of this conjugated path from the iron center to the nitro group. On the contrary, β decreases by 40% and 50% (for DPPE and (+)-DIOP compounds, respectively) upon insertion of a second phenyl ring. This can be explained by a breaking of the conjugation due to a significant torsion angle in the biphenyl linkage [11], which also fits with the blue-shift of the absorption band. After reduction to static values the trends in β are strongly reduced (see Table 2), showing the importance of the near-resonance effect between the electronic transition and the second harmonic wavelength. In fact, from the two-level model even the static β_0 values are expected to increase with increasing λ_{eg}, which is not observed in these compounds. However, the variation in λ_{eg} is relatively small and other factors, e.g. the change in dipole moment upon excitation (also occurring in the two-level model expression for β_0), are likely to vary more among the compounds.
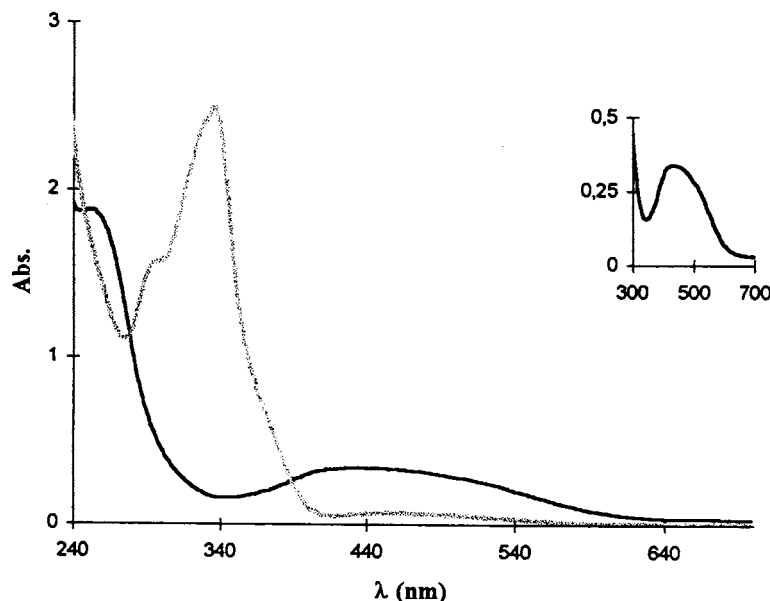
Fig. 2. UV–Vis absorption spectra of $[FeCp(DPPE)(p\text{-}N\equiv CC_6H_4NO_2)][PF_6]$ (——) and $[FeCp(DPPE)(p\text{-}N\equiv CC_6H_4N(CH_3)_2)][PF_6]$ (– – –) recorded in CH_2Cl_2 (ca. 1.5×10^{-4} mol dm^{-3}).

For a series of similar complexes (including cobalt, nickel and ruthenium analogs) studied previously [11], a very clear correlation was found between increasing β values and increasing wavelength and/or intensity of the lowest energy absorption band, attributed to the MLCT transition. This trend is continued in the present iron complexes, although for quantitative analysis the application of the two-level model must be questioned, taking into account that these compounds have their lowest energy transition due on resonance with the second harmonic wavelength.

Each of the DPPE compounds is found to possess a somewhat larger hyperpolarizability than the corresponding (+)-DIOP analog, in good agreement with the IR and NMR data, all together pointing out an increased electron density on the metal center for the DPPE compounds. However, the slight blue-shift in the optical absorption spectra of $[FeCp(DPPE)(p\text{-}NC(C_6H_4)_2NO_2)][PF_6]$ compared to its (+)-DIOP analog is not well understood. This increase in β is not affected by the resonance effect as it persists in the static values β_0, which indicates that more electronic density at the metal center is effectively contributing to the hyperpolarizability.

2.4. Molecular orbital calculations

In order to understand the geometric and electronic factors that may be conditioning the design of new compounds showing large hyperpolarizabilities, MO calculations were carried out on several model complexes.

Extended Hückel MO calculations (EHMO) (see Section 4.5) carried out on the model complexes $[FeCp(PH_3)_2(p\text{-}NCR)]^+$ (R = $C_6H_4NO_2$ or $C_6H_4C_6H_4NO_2$) show that the larger values of experimental hyperpolarizabilities correspond to lower HOMO–LUMO gaps. A simplified scheme (Fig. 4) of the interaction diagram between the metal center $[FeCp(PH_3)_2]^+$ and the $p\text{-}NCC_6H_4NO_2$ ligand shows that the HOMO of the complex is essentially localized in the metal fragment while the LUMO is essentially a pure ligand orbital. This scheme also depicts a π-backbonding interaction between the SHOMO (second HOMO) of the metal center (Fig. 5b) and an empty orbital of the ligand (Fig. 5a).

One interesting feature that can be observed is the contribution of the in-plane p orbital of the aryl *ortho* carbons perpendicular to the CC bond (Fig. 5a) and
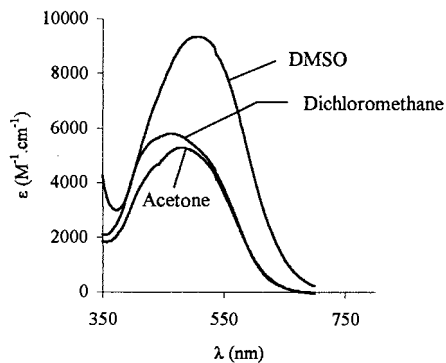

Fig. 3. Solvatochromic behavior of the MLCT band of $[FeCp(DPPE)((E)\text{-}p\text{-}NCC(H)=C(H)\text{-}C_6H_4NO_2)][PF_6]$ in solvents of different polarity.

Table 2
The experimental hyperpolarizability, β, measured by HRS at $\lambda_0 = 1064$ nm, for a selection of the ligands and the Fe(II) compounds; the static hyperpolarizability β_0 is obtained from the two-level model taking the transition corresponding to the long-wavelength absorption band, λ_{eg}

	β (10^{-30} esu)	β_0 (10^{-30} esu)	λ_{eg} (nm)
Fe(II) compounds			
$[FeCp((+)\text{-}DIOP)(p\text{-}NCC_6H_4NO_2)]^+$	380	86	454
$[FeCp(DPPE)(p\text{-}NCC_6H_4NO_2)]^+$	395 [a,b]	115	460
$[FeCp((+)\text{-}DIOP)(p\text{-}NCC_6H_4C_6H_4NO_2)]^+$	190	78	403
$[FeCp(DPPE)(p\text{-}NCC_6H_4C_6H_4NO_2)]^+$	240 [a]	108	372
$[FeCp((+)\text{-}DIOP)((E)\text{-}p\text{-}NCC(H)=C(H)C_6H_4NO_2)]^+$	520	105	466
$[FeCp(DPPE)((E)\text{-}p\text{-}NCC(H)=C(H)C_6H_4NO_2)]^+$	570	112	484
Ligands			
$p\text{-}NCC_6H_4NO_2$	4.4 [a]	3.2	257
$p\text{-}NCC_6H_4C_6H_4NO_2$	14.6 [a]	9.4	294

[a] Ref. [11].

[b] Corrected value: in ref. [11] a CH_2Cl_2 solvent molecule in the structure had been erroneously ommitted in the calculation of the molecular weight.

also, in the metallic fragment, the contribution of one of the Cp π orbitals (Fig. 5b).

Due to the anti-bonding character of the (a) orbital we can predict a lengthening of the NC bond with the corresponding observed decrease in the IR stretching frequency, when compared with the free ligand. Also the increase in charge density of the *ortho* carbons will induce the upfield shift in the NMR spectra leaving the *meta* carbons almost unchanged. This increase in charge density is derived from π-backdonation from the (b) orbital, involving also a contribution of Cp carbons, which could explain the deshielding observed for the Cp carbons.

Once understood that the best values of hyperpolarizabilities can be achieved with lower HOMO–LUMO gaps, and since these orbitals are nearly non-bonding orbitals of the metal center and p-NCR ligand respectively, we can improve the non-linear optics of our compounds by fine tuning the metal center with different stabilizing ligands (changing phosphines or replacing the Cp by indenyl or pyrrolyl ligands) aiming to raise the HOMO or by using other R groups leading to lower LUMOs. Because lower LUMOs (or higher HOMOs) will be better π acceptors (π donors) we can use, in this general family of compounds, the NMR chemical shifts of the *ortho* carbons in the R group as a probe to find compounds with potentially improved NLO properties.

To help in the design of new compounds, selecting the directions which the time consuming synthetic work should follow, we performed ab initio calculations to compute the static hyperpolarizability tensor components (see Section 4.5) of two model compounds and the corresponding conjugated ligands.

The influence of the extension of the basis set was tested with the free ligands p-$NCC_6H_4NO_2$ and p-

$NCC_6H_4C_6H_4NO_2$ which were fully optimized at STO-3G level and then the static hyperpolarizabilities were computed at STO-3G, 3-21G and 3-21G**. The results presented in Table 3 show that for the more sophisticated basis sets including contracted valence orbitals (3-21G and 3-21G**) the theoretical values are in very good agreement with the static hyperpolarizabilities derived from the experiment. In fact they are less than a factor two smaller, and the ratio between the values for the two ligands is quite well reproduced. Extension of the basis set to include polarization functions (3-21G**) does not yield any further improvement. The factor between the results with the STO-3G and the more complete basis sets is nearly the same for both conjugated ligands.

After the method had been tested in the free ligands, further calculations were carried out at HF-STO-3G level in two model iron complexes $[FeCp(PH_3)_2(p\text{-}NCR)]^+$ ($R = C_6H_4NO_2$ and $C_6H_4C_6H_4NO_2$) for comparison with the experimental results (see Table 4).
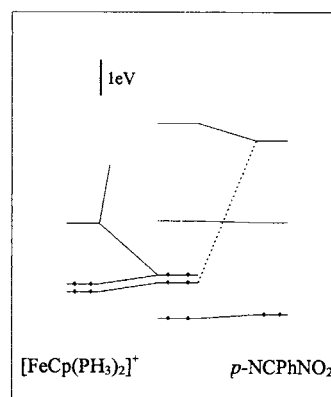

Fig. 4. Simplified interaction diagram between the metal center and the p-$NCC_6H_4NO_2$ ligand, showing the π-backbonding interaction as a dotted line.
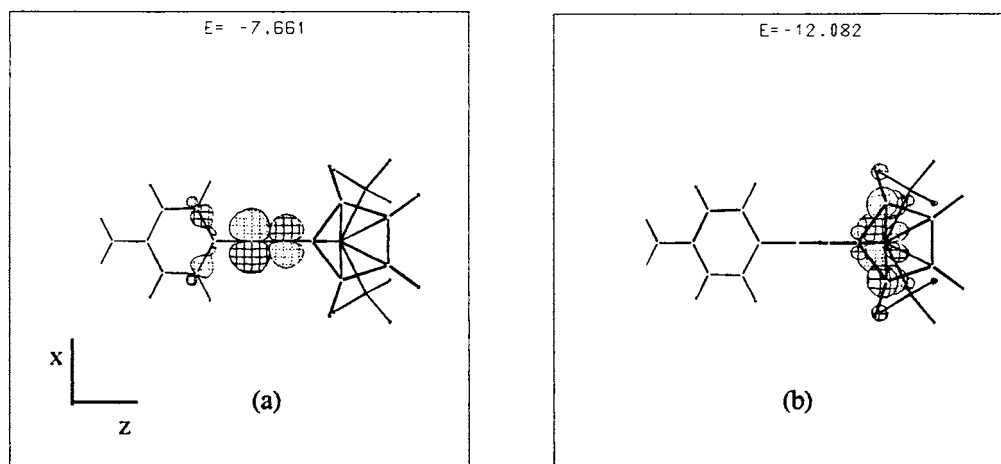
Fig. 5. Fragment orbitals involved in the π-backbonding interaction: (a) p-NCC$_6$H$_4$NO$_2$ ligand, (b) metal center.

Table 3
Comparison of calculated and experimental values of the static hyperpolarizability β_0 for the free ligands; the ratios are given between calculated results obtained from the largest and smallest basis sets

	β_0 (10^{-30} esu)				Factor
	Exp.	STO-3G	3-21G	3-21G**	STO-3G $\rightarrow$ 3-21G**
p-NCC$_6$H$_4$NO$_2$	3.2	0.77	2.42	2.40	3.1
p-NCC$_6$H$_4$C$_6$H$_4$NO$_2$	9.4	1.60	5.54	5.52	3.5

The results reproduce the trends in the experimental β_0 values quite well, apart from a systematic underestimation by a factor between 4.6 and 8.6. The latter is not unexpected, as even for the free ligands reducing the basis set from 3-21G** to STO-3G reduces the β_0 values by a factor of 3.1 to 3.5. One should also bear in mind here that in the calculation the electron-rich phosphines are replaced by simple PH$_3$ groups, which is a drastic simplification taking into account that the substitution of (+)-DIOP by DPPE already yields a sizeable increase (about 20–30%) of the static hyperpolarizabilities. Also rewarding is the observation of the same trend in the calculated and experimental values of decreasing β_0 from the phenyl to the biphenyl compound. This decrease is more important in the calculation (30% versus about 10% in the experiment) but the overall agreement is very good, taking into account the simplifications and approximations involved.

2.5. Crystallographic studies

While the focus of this work is the molecular optical non-linearities of the nitrile complexes, it was also of interest to examine crystal packing as an indicator of bulk material response, since a centrosymmetric arrangement in the lattice would spoil the bulk response of the SHG effect. With this in mind, a single X-ray

structural study of [FeCp(DPPE)(p-NCC$_6$H$_4$NO$_2$)]-[PF$_6$]·CH$_2$Cl$_2$ (**4**) was carried out to afford bond length data about the metal–nitrile linkage, to give solid-state packing information and to generate structural parameters (interatomic distances, angles) to be used in the molecular orbital calculations of the model complexes detailed above.

The molecular structure of [FeCp(DPPE)(p-NCC$_6$H$_4$NO$_2$)][PF$_6$]·CH$_2$Cl$_2$ (**4**) is shown in Fig. 6, along with the atom numbering scheme. The values of selected bond lengths and bond angles are given in Table 5. The structural study confirmed the presence of the PF$_6^-$ anion and revealed the presence of a solvent CH$_2$Cl$_2$ molecule of crystallization.

The metal is coordinated to the η^5-cyclopentadienyl ring, the two phosphorus atoms of the phosphine lig-

Table 4
Comparison of experimental static β_0 values with the HF-STO-3G results for the [FeCp(PH$_3$)$_2$(NCR)]$^+$ model complexes

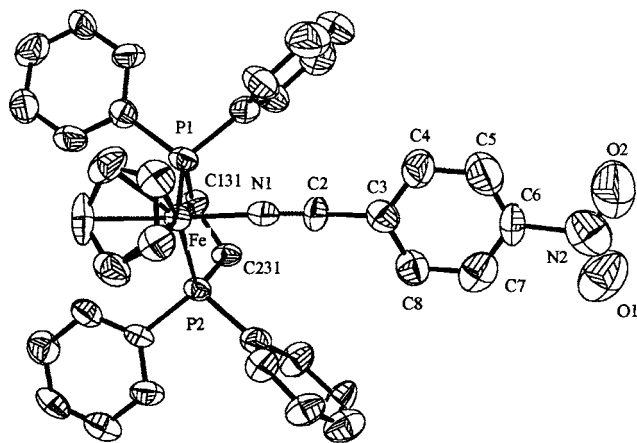|	β_0 (10^{-30} esu)	
	Exp.	STO-3G
[FeCp((+)-DIOP)(p-NCC$_6$H$_4$NO$_2$)]$^+$	86	18.3
[FeCp(DPPE)(p-NCC$_6$H$_4$NO$_2$)]$^+$	115	
[FeCp((+)-DIOP)(p-NCC$_6$H$_4$C$_6$H$_4$NO$_2$)]$^+$	78	12.6
[FeCp(DPPE)(p-NCC$_6$H$_4$C$_6$H$_4$NO$_2$)]$^+$	108	

Fig. 6. Diagram for **4**, [FeCp(DPPE)(p-N≡CC$_6$H$_4$NO$_2$)][PF$_6$], with 50% thermal ellipsoids, showing the labeling scheme. Hydrogen atoms have been omitted for clarity.

and and the nitrile nitrogen atom of the p-NCC$_6$H$_4$NO$_2$ ligand, showing the typical structure of cyclopentadienyl complexes in pseudo-octahedral three-legged piano stool geometry, on the assumption that the cyclopentadienyl group takes up three coordination sites.

The C(131)–P(1)–Fe–P(2)–C(231) chelate ring is not planar but exhibits an envelope conformation, i.e. the atoms Fe, P(1), P(2) and C(131) are essentially coplanar while atom C(231), the 'flap' atom of the envelope, lies more than −0.63(2) Å from this plane. As shown in Fig. 6, the non-planarity of this conformation diminishes the contacts between the chelate ring phenyl groups and the nitrile and cyclopentadienyl ligands.

The structural data permit comparisons, although the relative imprecision of the crystallographic determination of complex **4** necessitates caution in interpreting these data. A comparison between the coordination geometry about the Fe atom is given in Table 6 for reported structures of [FeCpL$_2$L′] (L$_2$ = DPPE, DPPM; L = CO, P(C$_6$H$_5$)$_3$, P(OCH$_3$)$_3$; L′ = NCCH$_3$, NCC$_6$H$_5$) complexes containing Fe–P or Fe–N≡C bonds. The phosphine structural data of compound **4**, i.e. Fe–P bond lengths 2.209 and 2.210 Å and P1–Fe–P2 angle 87.7° are similar to those in other FeCp derivatives containing DPPE and acetonitrile bonded ligands.

The Fe–N bond length (1.87 Å), being shorter than the corresponding distance found for some iron(II) complexes with acetonitrile ligand, is within crystallographic error similar to the Fe–N bond lengths of other FeCp(DPPE) complexes containing nitriles. Distances and angles within the benzonitrile group are consistent with the retention of aromaticity, in particular there is no obvious bond length alternation which would be expected for appreciable quinoidal contribution as was suggested by the spectroscopic IR and NMR data obtained for the complex. These features do

Table 5
Selected bond lengths [Å] and angles [°] for FeCp(DPPE)(p-N≡CC$_6$H$_4$NO$_2$)][PF$_6$]·CH$_2$Cl$_2$ (**4**)

Fe(1)–N(1)	1.874(11)	N(1)–Fe(1)–C(13)	157.1(5)
Fe(1)–C(13)	2.063(13)	N(1)–Fe(1)–C(14)	125.9(6)
Fe(1)–C(14)	2.088(14)	N(1)–Fe(1)–C(12)	126.1(6)
Fe(1)–C(12)	2.068(14)	N(1)–Fe(1)–C(15)	92.3(5)
Fe(1)–C(15)	2.090(13)	N(1)–Fe(1)–C(11)	93.3(5)
Fe(1)–C(11)	2.078(13)	N(1)–Fe(1)–P(1)	92.1(3)
Fe(1)–P(1)	2.210(4)	N(1)–Fe(1)–P(2)	86.6(3)
Fe(1)–P(2)	2.209(3)	P(1)–Fe(1)–P(2)	87.70(12)
Fe(1)–Centroid	1.721(7)	Centroid–Fe(1)–N(1)	122.3(8)
Fe(1)–Cp	−1.703(7)	Centroid–Fe(1)–P(1)	126.7(7)
P(1)–C(111)	1.816(13)	Centroid–Fe(1)–P(2)	129.2(8)
P(1)–C(121)	1.818(14)	C(111)–P(1)–Fe(1)	122.0(4)
P(1)–C(131)	1.866(13)	C(121)–P(1)–Fe(1)	113.9(5)
P(2)–C(231)	1.857(12)	C(131)–P(1)–Fe(1)	108.0(4)
P(2)–C(211)	1.829(11)	C(111)–P(1)–C(131)	102.3(6)
P(2)–C(221)	1.814(13)	C(121)–P(1)–C(131)	107.4(7)
N(1)–C(2)	1.129(14)	C(111)–P(1)–C(121)	101.9(6)
C(2)–C(3)	1.42(2)	C(231)–P(2)–C(211)	105.1(6)
C(3)–C(8)	1.35(2)	C(231)–P(2)–C(221)	103.4(6)
C(3)–C(4)	1.38(2)	C(211)–P(2)–C(221)	102.4(6)
C(4)–C(5)	1.39(2)	C(231)–P(2)–Fe(1)	107.3(4)
C(5)–C(6)	1.35(2)	C(211)–P(2)–Fe(1)	120.7(4)
C(6)–C(7)	1.33(2)	C(221)–P(2)–Fe(1)	116.1(4)
C(6)–N(2)	1.60(2)	C(2)–N(1)–Fe(1)	176.6(11)
C(7)–C(8)	1.37(2)	N(1)–C(2)–C(3)	177.4(15)
N(2)–O(1)	1.15(2)	O(1)–N(2)–O(2)	139(3)
N(2)–O(2)	1.16(2)	O(1)–N(2)–C(6)	112(2)
C(131)–C(231)	1.51(2)	O(2)–N(2)–C(6)	109(2)
		C(231)–C(131)–P(1)	109.9(8)
		C(131)–C(231)–P(2)	108.6(8)

not bring to evidence the existence of π-backdonation in the solid state. However, the nitrile group shows an almost linear geometry with Fe–N1–C2 and N1–C2–C3 angles of 177°, which indicate that the iron atom and the benzonitrile ligand are in the same plane and could stimulate the metal–ligand π-backdonation suggested by the spectroscopic data.

Unfortunately, the crystal packing of **4** is centrosymmetric due to crystallization in the orthorhombic space group *Pbcn* with eight independent molecules in the unit cell, making this compound unsuitable for macroscopic NLO purposes.

3. Concluding remarks

A series of iron(II) nitrile complexes, involving systematic variation in coligands, have been synthesized as model donor–acceptor systems to probe effects of structural variation on non-linear optical properties. Trends in spectroscopic and structural data and molecular quadratic hyperpolarizabilities have been examined. Spectroscopic data (IR, ^{1}H and ^{13}C-NMR) are sensitive to phosphine replacement, introduction of different *para*-substituent (nitro or dimethylamino group)

Table 6
Structural data for FeCp derivatives containing ligands with nitrogen or phosphorus donor atoms

Compound	Fe–Cp (Å)	Fe–P (Å)	P1–Fe–P2 (°)	Fe–N (Å)	N≡C (Å)	NC–C (Å)	Fe–N–C (°)	N≡C–C (°)	Reference
[FeCp(CO)$_2$(NCCH$_3$)][BF$_4$]	2.030			1.914	1.200	1.494	175.676	175.045	[16a]
	2.112								
[FeCp(CO)(PPh$_3$)(NCCH$_3$)]-[BF$_4$]	2.061	2.227		1.916	1.137	1.457	179.791	178.592	[16b]
	2.124								
[FeCp(P(OCH$_3$)$_3$)$_2$-(NCCH$_3$)][PF$_6$]	2.127	2.182	95.360	1.924	1.094	1.482	172.960	175.363	[16c]
	2.076	2.175							
[FeCp(DPPE)(NCCH$_3$)]-[BPh$_4$]	2.115	2.205	86.454	1.881	1.137	1.432	171.864	176.869	[16d]
	2.077	2.194							
[FeCp(DPPM)(NCCH$_3$)]-[PF$_6$]	2.046	2.196	74.673	1.892	1.135	1.438	179.591	178.146	[16e]
	2.090	2.207							
[Fe(AcCp)(DPPE)-(NCCH$_3$)][PF$_6$]	2.075	2.232	86.75	1.895	1.128	1.451	173.5	174.626	[16f]
	2.103	2.207							
[Fe(MeCp)(DPPE)-(NCCH$_3$)][PF$_6$]	2.103	2.218	86.311	1.905	1.133	1.456	177.322	178.611	[16g]
	2.126	2.237							
[Fe(DMPE)$_2$(NCC$_6$H$_5$)]-[PF$_6$]$_2$		2.260	84.835	1.888	1.149	1.433	174.64	174.72	[16h]
		2.277							
[Fe(DPPE)$_2$(NCCH$_3$)$_2$]-[BF$_4$]·CH$_2$Cl$_2$		2.320	83.197	1.913	1.141	1.467	177.908	179.094	[16i]
		2.342							
[FeCp(DPPE)-(p-NCC$_6$H$_4$NO$_2$)][PF$_6$]	2.063	2.209	87.70	1.874	1.129	1.42	176.6	177.4	This work
	2.090	2.210							
p-NCC$_6$H$_4$NO$_2$					1.155	1.438		179.2	[16j]

on nitrile ligand and nitrile chain-lengthening. Analysis of these data gives an insight in the role played by the organometallic moiety and the direction and extension of the π-delocalization on the complexes. The finding of an MLCT band in the electronic spectra of all nitro derivatives is in good agreement with the direction of this π-delocalization.

Accordingly, all the compounds measured by hyper-Rayleigh scattering, with DPPE or (+)-DIOP as phosphine ligand and an NO$_2$ acceptor group, presented significant NLO properties. It was found that β values increase with replacement of the (+)-DIOP coligand by the more donating DPPE bidentate phosphine and also with chromophore chain-lengthening. [FeCp-(DPPE)((E)-p-NCC(H)=C(H)C$_6$H$_4$NO$_2$)][PF$_6$] is found to have the highest β value (570×10^{-30} esu) in the series. The reduction to static hyperpolarizabilities shows that these values are resonance enhanced as could be expected from the close proximity of the MLCT band to the second harmonic wavelength.

Theoretical calculations depict a π-backbonding interaction between the SHOMO of the metal center and an empty orbital of the ligand. These results may also explain some ^{1}H and ^{13}C-NMR data found for the complexes: a shielding effect on the *ortho* carbons in the

nitrile ligand and a deshielding effect on Cp carbons. Therefore, in this family of compounds, NMR chemical shifts of the *ortho* positions can be used as a probe to search for compounds with potentially improved NLO properties as was suggested in our previous work [6,7].

The good agreement between the β_0 values derived from the experiment and those calculated theoretically at HF-STO-3G level encourages the future use of this calculation for prediction of static hyperpolarizabilities.

Moreover, the good correlation found between the spectroscopic studies and the experimental second-order non-linearities for some of the studied complexes, indicates that IR and NMR data can be used as a tool to predict non-linear optical behavior in solution, and therefore are useful as a probe to plan new synthetic strategies and to tune the non-linear optical behavior of these families of compounds.

X-ray structural study carried out for the promising compound [FeCp(DPPE)(p-NCC$_6$H$_4$NO$_2$)][PF$_6$] gave no evidence for a significant vinylidene contribution on the ground state geometry as would be expected from the spectroscopic data. Since this compound crystallizes on a centrosymmetric space group *Pbcn*, it is not suitable for application as an NLO crystal. However,

considering that the spectroscopic data indicate a similar electronic behavior for the DPPE and (*R*)-PROPHOS complexes, the use of this chiral phosphine can constitute a strategy for further studies on macroscopic NLO properties.

4. Experimental

4.1. General procedures

All experiments were carried out under dinitrogen or argon by use of standard Schlenk techniques. Solvents were dried according to the usual published methods [17]. (*S*)-PROLOPHOS was prepared following the literature [18]. DPPE and (*R*)-PROPHOS were used as purchased from Aldrich Chemical Co.

Solid state IR spectra were recorded on a Perkin Elmer 683 spectrophotometer in KBr pellets; only significant bands are cited in the text. ^1H, ^{13}C and the ^{31}P-NMR spectra were recorded on a Varian Unity 300 spectrometer at probe temperature. The UV–Vis spectra were taken on a Shimadzu 1202 spectrophotometer. Microanalyses were performed in our laboratories using a Fisons Instruments EA1108 system. Data acquisition, integration and handling were performed using a PC with the software package Eager-200 (Carlo Erba Instruments). Melting points were obtained on a Reichert Thermovar. The molar conductivities of 10^{-3} mol 1^{-1} solutions of the complexes in nitromethane were recorded with a Schott CGB55 Konduktometer.

The ^1H (acetone-d_6 and chloroform-d) and ^{13}C (chloroform-d) chemical shifts are reported in parts per million downfield from internal Me_4Si and the ^{31}P-NMR spectra are reported in parts per million downfield from external 85% H_3PO_4. Spectral assignments follow the numbering scheme shown in Fig. 7.

^1H- and ^{13}C-NMR data are similar for all the complexes containing the same phosphine. (*S*)-PROLOPHOS: ^1H-NMR ($(CD_3)_2CO$): 1.49 (m, 1H, CH_2); 1.69 (m, 2H, CH_2); 1.86 (m, 1H, CH_2); 2.20 (m, 1H, CH_2); 2.74 (m, 1H, CH_2); 3.17 (m, 1H, CH_2); 3.62 (m, 1H, CH); 3.86 (m, 1H, CH_2); 4.08 (m, 1H, CH_2); 6.68 (t, 2H, C_6H_5); 7.21 (q, 3H, C_6H_5); 7.34 (t, 1H, C_6H_5); 7.61–7.90 (cm, 14H, C_6H_5); 8.09 (t, 2H, C_6H_5). $^{13}C\{^1H\}$-NMR ($CDCl_3$): 25.60 (CH_2); 28.82 (CH_2); 49.86 (CH_2); 57.35 (CH); 70.14 (CH_2); 127.84–133.40 (C_6H_5); 136.80 (C-ipso, C_6H_5); 139.80 (C-ipso, C_6H_5).

(*R*)-PROPHOS: ^1H-NMR ($(CD_3)_2CO$): 1.20 and 1.23 (3H, dd, $J_{HH} = 6.6$, CH_3); 2.29 (m, 1H, CH_2), 2.44 (1H, br.s, CH); 3.28 and 3.44 (1H, dm, CH_2); 7.49–7.71 (16H, m, C_6H_5); 7.84 (2H, t, C_6H_5); 8.11 (2H, t, C_6H_5). $^{13}C\{^1H\}$-NMR ($CDCl_3$): 16.34 (CH_3); 31.92 (m, CH_2); 34.76 (m, CH); 128.90–133.96 (C_6H_5); 135.96 (d, $J_{CP} = 43.52$, C-ipso, C_6H_5).

DPPE: ^1H-NMR ($(CD_3)_2CO$): 2.46 (m, 2H, CH_2); 2.67 (m, 2H, CH_2); 7.35 (m, 4H, C_6H_5); 7.54 (q, 12H, C_6H_5); 7.85 (m, 4H, C_6H_5). $^{13}C\{^1H\}$-NMR ($CDCl_3$): 22.71 (t, CH_2, $J_{CP} = 21.40$); 130.97 (C-meta, C_6H_5); 131.23 (C-para, C_6H_5); 132.86 (C-ortho, C_6H_5, $^2J_{CP} = 23.20$); 136.59 (C-ipso, $J_{CP} = 18.33$).

4.2. Preparation of [FeCp(P_P)(I)]

[FeCp(*S*)-PROLOPHOS)(I)] was prepared following the procedure described previously [19]. [FeCp-(DPPE)(I)] and [FeCp((*R*)-PROPHOS)(I)] were prepared following the procedure: a boiling mixture of the iodide [FeCp(CO)$_2$(I)] (1 mmol) and (*R*)-PROPHOS (1.2 mmol) in benzene (50 ml) was irradiated, with stirring, with UV light for 30 min. Then the solvent was evaporated to dryness and the resulting solid washed three times with 20 ml of light petroleum (b.p. 30–40°C). The pure complex was obtained after a further recrystallization from dichloromethane–light petroleum (b.p. 60–80°C).

[FeCp((*S*)-PROLOPHOS)(I)]: dark-violet; 48% yield; m.p. 140–142°C, Anal. Calc. for $C_{34}H_{34}FeINOP_2$: C, 56.92; H, 4.77; N, 1.95. Found: C, 56.73; H, 4.87; N, 1.86%. ^1H-NMR (CD_2Cl_2): 1.18 (2H, m, CH_2); 1.81 (1H, m, CH_2); 2.59 (1H, m, CH_2); 3.03 (1H, m, CH_2); 3.44 (1H, m, CH); 3.65 (1H, m, CH_2); 3.85 (5H, s, η^5-C_5H_5), 4.56 (1H, m, CH_2); 6.45 (2H, d, C_6H_5); 6.99 (2H, t, C_6H_5); 7.17 (4H, m, C_6H_5); 7.46 (10H, m, C_6H_5); 8.12 (1H, br.s, C_6H_5); 8.27 (1H, br.s, C_6H_5).

[FeCp((*R*)-PROPHOS)(I)]: anthracite; 80% yield; m.p. 142°C (dec.) Anal. Calc. for $C_{32}H_{31}FeIP_2$: C, 58.21; H, 4.73. Found: C, 57.91; H, 4.71%. ^1H-NMR ($CDCl_3$): 1.12 (3H, br.s, CH_3); 1.96 (1H, m, CH_2); 2.57 (1H, m, CH); 3.15 (1H, m, CH_2); 4.16 (5H, s, η^5-C_5H_5); 7.15 (2H, m, C_6H_5); 7.35 (14H, m, C_6H_5); 7.64 (2H, m, C_6H_5); 8.06 (2H, m, C_6H_5).

4.3. Preparation of [FeCp(P_P)(p-NCC$_6$H$_4$R)][PF$_6$]

[FeCp((+)-DIOP)(p-NCR)][PF] (R = C_6H_4N-$(CH_3)_2$, $C_6H_4NO_2$, $C_6H_4C_6H_4NO_2$, (*E*)-C(H)=C(H)-$C_6H_4NO_2$) synthesis and characterization was described previously [6]. Some spectroscopic data of these compounds are also introduced in order to make comparisons with the phosphine derivatives studied in this work.

All the other complexes were prepared by the process described below. To a solution of [FeCp(P_P)(I)] (1 mmol) and the appropriate nitrile p-NCR (R = $C_6H_4N(CH_3)_2$, $C_6H_4NO_2$, (*E*)-C(H)=C(H)$C_6H_4NO_2$, $C_6H_4C_6H_4NO_2$) (2 mmol) in dichloromethane (40 ml) was added TlPF$_6$ (1 mmol) at room temperature. The mixture was stirred at room temperature for 12–20 h. A change was observed from dark-violet to orange or red with simultaneous precipitation of thallium iodide.

After filtration, the solution was evaporated under vacuum to dryness and washed several times with ether to remove the excess of nitrile. The residue was recrystallized from dichloromethane–ether.

[FeCp((S)-PROLOPHOS)(p-NCC$_6$H$_4$N(CH$_3$)$_2$)][PF$_6$] (**1**): dark orange; 68% yield, m.p. 198°C (dec.). Anal. Calc. for C$_{43}$H$_{44}$F$_6$FeN$_3$OP$_3$: C, 58.58; H, 5.03; N, 4.76. Found: C, 58.67; H, 5.18; N, 4.62%. IR (KBr): v(CN) 2210 cm^{-1}. ^{1}H-NMR ((CD$_3$)$_2$CO): 3.08 (s, 6H, N(CH$_3$)$_2$); 4.23 (s, 5H, η^5-C$_5$H$_5$); 6.78 (d, 2H, J_{HH} = 8.9, H$_3$,H$_5$); 7.41 (d, 2H, J_{HH} = 9.2, H$_2$,H$_6$). ^{13}C{^{1}H}-NMR (CDCl$_3$): 39.85 (N(CH$_3$)$_2$); 81.72 (η^5-C$_5$H$_5$); 95.94 (C1); 111.83 (C3,C5); (C2,C6) (signal obscured by the aromatic carbons of phosphine); (CN) (signal obscured by the aromatic carbons of phosphine); 153.05 (C4).

[FeCp((S)-PROLOPHOS)(p-NCC$_6$H$_4$NO$_2$)][PF$_6$] (**2**): red; 59% yield, m.p. 208°C (dec.). Anal. Calc. for C$_{41}$H$_{38}$F$_6$FeN$_3$O$_3$P$_3$·CH$_2$Cl$_2$: C, 52.08; H, 4.16; N, 4.34. Found: C, 51.97; H, 4.63; N, 3.81%. IR (KBr): v(CN) 2210, v(NO$_2$) 1525, 1345 cm^{-1}. ^{1}H-NMR ((CD$_3$)$_2$CO): 4.40 (s, 5H, η^5-C$_5$H$_5$); 7.99 (d, 2H, J_{HH} = 8.6, H$_2$,H$_6$); 8.41 (d, 2H, J_{HH} = 8.6, H$_3$,H$_5$). ^{13}C{^{1}H}-NMR (CDCl$_3$): 83.14 (η^5-C$_5$H$_5$); 118.80 (C1); 124.58 (C3,C5); (CN) (signal obscured by the aromatic carbons of phosphine); 133.69 (C2,C6); 149.50 (C4). ^{31}P{^{1}H}-NMR (CDCl$_3$): 111.40 (d, J_{PP} = 91.07, P(N)); 174.58 (d, J_{PP} = 91.7, P(O)).

[FeCp(DPPE)(p-NCC$_6$H$_4$N(CH$_3$)$_2$)][PF$_6$] (**3**): brick orange; 92% yield, m.p. 208–210°C. Anal. Calc. for C$_{40}$H$_{39}$F$_6$FeN$_2$P$_3$: C, 59.27; H, 4.85; N, 3.45. Found: C, 58.72; H, 5.20; N, 3.47%. IR (KBr): v(CN) 2210 cm^{-1}. ^{1}H-NMR ((CD$_3$)$_2$CO): 2.97 (s, 6H, N(CH$_3$)$_2$); 4.59 (s, 5H, η^5-C$_5$H$_5$); 6.38 (d, 2H, J_{HH} = 9.0, H$_3$,H$_5$); 6.47 (d, 2H, J_{HH} = 9.3, H$_2$,H$_6$). ^{13}C{^{1}H}-NMR (CDCl$_3$): 39.72 (N(CH$_3$)$_2$); 78.99 (η^5-C$_5$H$_5$); 95.67 (C1); 111.00 (C3,C5); 130.52 (C2,C6); (CN) (signal obscured by the aromatic carbons of phosphine); 152.29 (C4). ^{31}P{^{1}H}-NMR (CDCl$_3$): 96.31.

Fig. 7. Numbering scheme for NMR spectral assignments.

[FeCp(DPPE)(p-NCC$_6$H$_4$NO$_2$)][PF$_6$] (**4**): violet; 52% yield, m.p. 110°C (dec.). Anal. Calc. for C$_{38}$H$_{33}$F$_6$FeN$_2$O$_2$P$_3$: C, 56.18; H, 4.09; N, 3.45. Found: C, 55.73; H, 4.54; N, 3.21%. IR (KBr): v(CN) 2205, v(NO$_2$) 1520, 1340 cm^{-1}. ^{1}H-NMR ((CD$_3$)$_2$CO): 4.72 (s, 5H, η^5-C$_5$H$_5$); 6.97 (d, 2H, J_{HH} = 9.0, H$_2$,H$_6$); 8.11 (d, 2H, J_{HH} = 9.3, H$_3$,H$_5$). ^{13}C{^{1}H}-NMR (CDCl$_3$): 80.42 (η^5-C$_5$H$_5$); 116.93 (C1); 123.69 (C3,C5); 129.91 (CN); 131.01 (C2,C6); 149.05 (C4). ^{31}P{^{1}H}-NMR (CDCl$_3$): 98.09.

[FeCp(DPPE)(p-NCC(H)=C(H)C$_6$H$_4$NO$_2$)][PF$_6$] (**5**): violet; 45% yield, m.p. 221°C (dec.). Anal. Calc. for C$_{40}$H$_{35}$F$_6$FeN$_2$O$_2$P$_3$: C, 57.30; H, 4.21; N, 3.34. Found: C, 56.94; H, 4.06; N, 3.16%. IR (KBr): v(CN) 2205, v(NO$_2$) 1520, 1345 cm^{-1}. ^{1}H-NMR ((CD$_3$)$_2$CO): 4.65 (s, 5H, η^5-C$_5$H$_5$); 5.95 (d, 1H, J_{HH} = 17.1, H$_8$); 6.52 (d, 1H, J_{HH} = 16.5, H$_7$); 7.61 (d, 2H, J_{HH} = 8.4, H$_2$,H$_6$); 8.19 (d, 2H, J_{HH} = 8.4, H$_3$,H$_5$). ^{13}C{^{1}H}-NMR (CDCl$_3$): 80.12 (η^5-C$_5$H$_5$); 99.75 (C8); 124.08 (C3,C5); 128.18 (C2,C6); 130.43 (CN); 139.17 (C1); 147.64 (C7); 148. 62 (C4). ^{31}P{^{1}H}-NMR (CDCl$_3$): 97.64.

[FeCp(DPPE)(p-NCC$_6$H$_4$C$_6$H$_4$NO$_2$)][PF$_6$] (**6**): orange; 84% yield, m.p. 220–222°C. Anal. Calc. for C$_{44}$H$_{37}$F$_6$FeN$_2$O$_2$P$_3$·CH$_2$Cl$_2$: C, 55.52; H, 4.04; N, 2.88. Found: C, 55.84; H, 3.95; N, 2.87%. IR (KBr): v(CN) 2205, v(NO$_2$) 1515, 1350 cm^{-1}. ^{1}H-NMR ((CD$_3$)$_2$CO): 4.69 (s, 5H, η^5-C$_5$H$_5$); 6.83 (d, 2H, J_{HH} = 8.7, H$_2$,H$_{12}$); 7.73 (d, 2H, J_{HH} = 7.8, H$_3$,H$_{11}$); 7.90 (d, 2H, J_{HH} = 9.0, H$_6$,H$_{10}$); 8.31 (d, 2H, J_{HH} = 9.0, H$_7$,H$_9$). ^{13}C{^{1}H}-NMR (CDCl$_3$): 79.75 (η^5-C$_5$H$_5$); 111.16 (C1); 124.12 (C7,C9); 127.69 (C3,C11); 128.42 (C6,C10); (CN) (signal obscured by the aromatic carbons of phosphine); 132.41 (C2,C12); 142.75 (C4); 144.95 (C5); 147.64 (C8). ^{31}P{^{1}H}-NMR (CDCl$_3$): 96.02.

[FeCp((R)-PROPHOS)(p-NCC$_6$H$_4$N(CH$_3$)$_2$)][PF$_6$](**7**): red; 92% yield, m.p. 135–137°C. Anal. Calc. for C$_{41}$H$_{41}$F$_6$FeN$_2$P$_3$: C, 59.51; H, 4.99; N, 3.40. Found: C, 60.04; H, 5.22; N, 3.09%. IR (KBr): v(CN) 2210 cm^{-1}. ^{1}H-NMR ((CD$_3$)$_2$CO): 2.99 (s, 6H, N(CH$_3$)$_2$); 4.49 (s, 5H, η^5-C$_5$H$_5$); 7.48 (d, 2H, J_{HH} = 9.6, H$_3$,H$_5$); 7.64 (d, 2H, J_{HH} = 8.1, H$_2$,H$_6$). ^{13}C{^{1}H}-NMR (CDCl$_3$): 39.78 (N(CH$_3$)$_2$); 79.22 (η^5-C$_5$H$_5$); 95.69 (C1); 110.99 (C3,C5); 131.12 (C2,C6); (CN) (signal obscured by the aromatic carbons of phosphine); 152.59 (C4). ^{31}P{^{1}H}-NMR (CDCl$_3$): 82.45 (d, J_{PP} = 44.4); 106.64 (d, J_{PP} = 45.1).

[FeCp((R)-PROPHOS)(p-NCC$_6$H$_4$NO$_2$)][PF$_6$] (**8**): violet; 96% yield, m.p. 236°C (dec.). Anal. Calc. for C$_{39}$H$_{35}$F$_6$FeN$_2$O$_2$P$_3$: C, 56.47; H, 4.25; N, 3.38. Found: C, 56.37; H, 4.22; N, 3.23%. IR (KBr): v(CN) 2210, v(NO$_2$) 1515, 1340 cm^{-1}. ^{1}H-NMR ((CD$_3$)$_2$CO): 4.65 (s, 5H, η^5-C$_5$H$_5$); 7.10 (d, 2H, J_{HH} = 8.7, H$_2$,H$_6$); 8.12 (d, 2H, J_{HH} = 8.7, H$_3$,H$_5$). ^{13}C{^{1}H}-NMR (CDCl$_3$): 80.48 (η^5-C$_5$H$_5$); 116.98 (C1); 123.70 (C3,C5); (CN) (signal obscured by the aromatic carbons of phosphine); 133.14 (C2,C6); 148.99 (C4). ^{31}P{^{1}H}-NMR (CDCl$_3$): 81.89 (d, J_{PP} = 43.6); 104.54 (d, J_{PP} = 43.1).
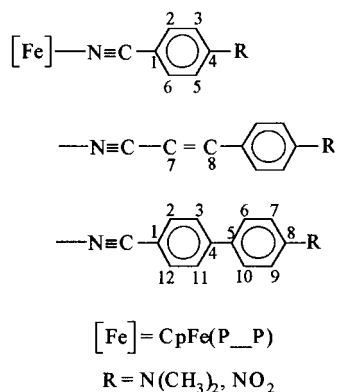
4.4. β Measurements

Hyper-Rayleigh scattering (HRS) measurements were performed using 70 ps pulses from a Nd:YAG regenerative amplifier ($\lambda = 1064$ nm) operating at a repetition rate of 2 kHz. A detailed description of the experimental procedure has been given in refs. [11,20]. In this setup, any erroneous signals due to the two photon luminescence are adequately eliminated by systematically scanning a narrow region around the second harmonic wavelength using a monochromator and to some extent also by using a nanosecond electronic time gating. Hyperpolarizabilities are determined from the HRS intensity by internal reference relative to chloroform. The intensity of the HRS light is proportional to the concentration and to the orientational averages $\langle \beta_{ZZZ}^2 \rangle$ and $\langle \beta_{XZZ}^2 \rangle$ (upper case indices: laboratory coordinates) of the molecular hyperpolarizability, for the polarization components parallel and orthogonal to the polarization of the incident laser beam, respectively. For simplicity we assume that the β tensors of both solvent and solute molecules are dominated by a single (diagonal) tensor component β_{zzz} (lower case indices: molecular coordinates). For the present NLO compounds, this is expected to be a very good approximation, as previous measurements [11] on similar complexes all showed depolarization ratios $\langle \beta_{XZZ}^2 \rangle / \langle \beta_{ZZZ}^2 \rangle$ very close to 0.2, and the theoretical prediction $\langle \beta_{XZZ}^2 \rangle / \langle \beta_{ZZZ}^2 \rangle = 1/5$ is also exactly reproduced by our HF-STO-3G calculations on the Fe(II) model compounds. Also, with the proper choice of the molecular z-direction, the theoretical calculations β_{zzz} value is at least 15 times larger than any other tensor component. With this assumption, the orientational averages are given by $\langle \beta_{ZZZ}^2 \rangle = \frac{1}{7}\beta_{zzz}^2$ and $\langle \beta_{XZZ}^2 \rangle = \frac{1}{35}\beta_{zzz}^2$, and therefore β_{HRS}, defined as $(\langle \beta_{ZZZ}^2 \rangle + \langle \beta_{XZZ}^2 \rangle)^{1/2}$ ($\propto$ total HRS intensity), is equal to $\sqrt{6/35}\beta_{zzz}$. In this way, the ratio β_{HRS}(solute)/β_{HRS}(CHCl$_3$) obtained from the experiments can be directly interpreted as the ratio of the molecular zzz-components and β_{zzz}(solute) is obtained by adopting a value of 0.49×10^{-30} esu for $|\beta_{zzz}(\text{CHCl}_3)|$ (EFISHG, from ref. [21]). Although for CHCl$_3$ significant off-diagonal components may be expected, additional assumptions on the tensor components would be needed to improve on this analysis.

4.5. Molecular orbital calculations

Combined ab initio and extended Hückel calculations were carried out on model complexes. Ab initio calculations were performed at Hartree–Fock level using the GAUSSIAN94/DFT program [22]. Extended Hückel [23] type calculations with modified H_{ij} values [24] were also carried out. The basis set for the metal atoms consisted of ns, np and $(n-1)$d orbitals. The s and p orbitals were described by single Slater type wave func-

tions, and d orbitals were taken as contracted linear combinations of two Slater type wave functions. Standard parameters were used for all atoms. All MO drawings were made with CACAO [25]. The crystal structure of the organometallic complex [FeCp(DPPE)-(p-NCC$_6$H$_4$NO$_2$)][PF$_6$]·CH$_2$Cl$_2$ was used as starting model for all calculations. In all ab initio calculations the phosphines were replaced by PH$_3$ groups.

The β_{ijk} components of the static hyperpolarizability (10 independent components for this symmetrical tensor) were determined from ab initio calculations, in order to obtain the orientationally averaged observables $\langle \beta_{ZZZ}^2 \rangle$ and $\langle \beta_{XZZ}^2 \rangle$, following the formulae described by Cyvin et al. [26]. This eventually yields the depolarization ratio as $\beta_{XZZ}^2 / \beta_{ZZZ}^2$. The intensity of the unpolarized second harmonic scattering is proportional to $\beta_{HRS} = (\langle \beta_{ZZZ}^2 \rangle + \langle \beta_{XZZ}^2 \rangle)^{1/2}$, and the reported β_0 is an effective β_{zzz} value computed as $\beta_0 = \sqrt{35/6}\beta_{HRS}$.

4.6. X-ray structure of [FeCp(DPPE)-(p-N≡CC$_6$H$_4$NO$_2$)][PF$_6$]·CH$_2$Cl$_2$

Crystal data: [C$_{38}$H$_{31}$F$_6$N$_2$O$_2$P$_3$Fe.CH$_2$Cl$_2$], M_r 895.33, orthorhombic, space group *Pbcn*, $a = 12.928(2)$, $b = 29.9820(10)$, $c = 21.725(2)$ Å, $V = 8420.8$ Å^3, $D_{calc} = 1.412$ Mg m^{-3}, $Z = 8$, $\lambda(\text{Mo-K}_\alpha) = 0.71069$ Å, $\mu(\text{Mo-K}_\alpha) = 0.661$ mm^{-1}. Data were collected at 293(2) K on an Enraf–Nonius TURBOCAD4 diffractometer. The unit cell dimensions and orientation matrix were obtained by least-squares refinement of 25 centered reflections with $13 < \theta < 16°$. Using the CAD4 software, data were corrected for Lorentz and polarization effects and empirically for absorption. Intensities of 7416 reflections (7416 unique reflections) in the range $1.65 \leq \theta \leq 24.99°$ were measured by the ω–2θ scan mode. The structure was solved with SHELXS-86 [27] and refined by full-matrix least-squares method with SHELX93 [28]. 5607 reflections with $F > 3\sigma(F)$ were used in the structure solution and the final $R(F)$ value was 0.1172, for 511 refined parameters.

Non-hydrogen atoms were anisotropically refined and all hydrogen atoms were inserted in calculated positions and refined isotropically with a thermal parameter equal to 1.2 times those of the atoms to which they are bonded. A solvent molecule, CH$_2$Cl$_2$, was found to be disordered over two positions. The occupation factors refined 0.75 and 0.25 values used in the last cycle of refinement. In the disorder model the C–Cl distances were restrained to 1.75 Å and the thermal parameters were restrained to be approximately isotropic with an e.s.d. of 0.005 (ISOR). Two half molecules of PF$_6$ were found to be in a two-fold axis. The thermal parameters of the fluorine atoms in one of them were also refined with ISOR (e.s.d. of 0.005). The thermal parameters of the oxygen atoms of the nitrile ligand were also restrained (e.s.d. 0.01). The largest

peak in the final difference Fourier synthesis, 0.937 e. Å^{-3}, was found near the *F* atoms of one of the PF_6 molecules. The illustrations were drawn with program ORTEP-II [29]. The atomic scattering factors and anomalous scattering terms were taken from international tables [30].

5. Supplementary material

Crystallographic data for the structural analysis of compound **4**, [FeCp(DPPE)(*p*-NCC$_6$H$_4$NO$_2$)][PF$_6$] have been deposited with the Cambridge Crystallographic Data Centre, CCDC no. 145093. Copies of this information may be obtained free of charge from The Director, CCDC, 12 Union Road, Cambridge, CB2 1EZ, UK (Fax: + 44-1223-336033; e-mail: deposit@ccdc.cam.ac. uk or www: http://www.ccdc.cam.ac.uk).

References

[1] D.S. Chemla, J. Zyss (Eds.), Nonlinear Optical Properties of Organic Molecules and Crystals, vols. 1 and 2, Academic Press, Orlando, FL, 1987.

[2] S.R. Marder, J.E. Sohn, G.D. Stucky (Eds.), Materials for Nonlinear Optics: Chemical Perspectives, American Chemical Society Press, Washington, DC, 1991, ACS Symp. Ser. 455.

[3] D.J. Williams, Angew. Chem. Int. Ed. Engl. 23 (1984) 690.

[4] J. Zyss (Ed.), Molecular Nonlinear Optics: Materials, Physics, and Devices, Academic Press, San Diego, CA, 1994.

[5] (a) H.S. Nalwa, Appl. Organomet. Chem. 5 (1991) 349. (b) I.R. Whittall, A.M. McDonagh, M.G. Humphrey, M. Samoc, Adv. Organomet. Chem. 42 (1998) 291 and refs. cited therein. (c) J. Qin, D. Liu, C. Daí, C. Chen, B. Wu, C. Yang, C. Zhen, Coord. Chem. Rev. 188 (1999) 23. (d) I.R. Whittall, M.P. Cifuentes, M.G. Humphrey, B. Luther-Davies, M. Samoc, S. Houbrechts, A. Persoons, G.A. Heath, D.C.R. Hockless, J. Organomet. Chem. 549 (1997) 127. (e) S. Houbrechts, C. Boutton, K. Clays, A. Persoons, I.R. Whittall, R.H. Naulty, M.P. Cifuentes, M.G. Humphrey, J. Nonlinear Opt. Phys. Mater. 7 (1998) 113. (f) E. Goovaerts, W.E. Wenseleers, M.H. Garcia, G.H. Cross, Design and characterisation of organic and organometallic molecules for second order nonlinear optics. In: H.S. Nalwa (Ed.), Handbook of Advanced Electronic and Photonic Materials, Academic Press, New York, in press.

[6] A.R. Dias, M. Helena Garcia, M. Paula Robalo, M.L.H. Green, K.K. Lai, A.J. Pulham, S.M. Klueber, G. Balavoine, J. Organomet. Chem. 453 (1993) 241.

[7] A.R. Dias, M. Helena Garcia, J.C. Rodrigues, M.L.H. Green, S.M. Klueber, J. Organomet. Chem. 475 (1994) 241.

[8] A.R. Dias, M.H. Garcia, P.J. Mendes, M.P. Robalo, J.C. Rodrigues, Trends Organomet. Chem. 1 (1994) 335.

[9] (a) M. Paula Robalo, PhD Thesis, FCUL, Lisbon, 1992. (b) J. Manuel Rodrigues, PhD Thesis, FCUL, Lisbon, 1999.

[10] J.C. Calabrese, L.-T. Cheng, J.C. Green, S.R. Marder, W. Tam, J. Am. Chem. Soc. 113 (1991) 7227.

[11] W. Wenseleers, A.W. Gerbrandij, E. Goovaerts, M.H. Garcia, M.P. Robalo, P.J. Mendes, J.C. Rodrigues, A.R. Dias, J. Mater. Chem. 8 (1998) 925.

[12] W.J. Geary, Coord. Chem. Rev. 7 (1977) 81.

[13] K. Clays, A. Persoons, Phys. Rev. Lett. 66 (1991) 2980.

[14] K. Clays, A. Persoons, Rev. Sci. Instrum. 63 (1992) 3285.

[15] R.W. Terhune, P.D. Maker, C.M. Savage, Phys. Rev. Lett. 14 (1965) 681.

[16] (a) S. Fadel, K. Weidenhammer, M.L. Ziegler, Z. Anorg. Allg. Chem. 453 (1979) 98. (b) A.G.M. Barrett, N.E. Carpenter, M. Sabat, J. Organomet. Chem. 352 (1988) C8. (c) H. Schumann, L. Eguren, J.W. Ziller, J. Organomet. Chem. 408 (1991) 361. (d) P.E. Riley, C.E. Capshew, R. Pettit, R.E. Davis, Inorg. Chem. 17 (1978) 408. (e) J. Ruiz, M.-T. Garland, E. Roman, D. Astruc, J. Organomet. Chem. 377 (1989) 309. (f) J. Ruiz, M.A. Gonzalez, E. Roman, M.T. Garland, J. Chem. Soc. Chem. Commun. (1990) 21. (g) J. Ruiz, D. Astruc, J.P. Bideau, M. Cotrait, Acta Crystallogr. Sect. C 46 (1990) 2367. (h) A.V. George, L.D. Field, E.Y. Malouf, A.E.D. McQueen, S.R. Pike, G.R. Purches, T.W. Hambley, I.E. Buys, A.H. White, D.C.R. Hockless, B.W. Skelton, J. Organomet. Chem. 538 (1997) 101. (i) A.J. Blake, A.J. Atkins, R.O. Gould, M. Schroder, Z. Kristallogr. 198 (1992) 287. (j) T. Higashi, K. Osaki, Acta Crystallogr. Sect. B 33 (1977) 2337.

[17] D.D. Perrin, W.L.F. Amarego, D.R. Perrin, Purification of Laboratory Chemicals, Pergamon, New York, 2nd edn., 1980.

[18] E. Cesarotti, A. Chiesa, G. Ciani, A. Sironi, J. Organomet. Chem. 251 (1983) 79.

[19] G. Balavoine, M.L.H. Green, J.P. Sauvage, J. Organomet. Chem. 128 (1977) 247.

[20] M. Szablewski, P.R. Thomas, A. Thornton, D. Bloor, G.H. Cross, J.M. Cole, J.A.K. Howard, M. Malagoli, F. Meyers, J.-L. Brédas, W. Wenseleers, E. Goovaerts, J. Am. Chem. Soc. 119 (1997) 3144.

[21] F. Kajzar, I. Ledoux, J. Zyss, Phys. Rev. A 36 (1987) 2210.

[22] M.J. Frisch, G.W. Trucks, H.B. Schlegel, P.M.W. Gill, B.G. Johnson, M.A. Robb, J.R. Cheeseman, T. Keith, G.A. Petersson, J.A. Montgomery, K. Raghavachari, M.A. Al-Laham, V.G. Zakrzewski, J.V. Ortiz, J.B. Foresman, J. Cioslowski, B.B. Stefanov, A. Nanayakkara, M. Challacombe, C.Y. Peng, P.Y. Ayala, W. Chen, M.W. Wong, J.L. Andres, E.S. Replogle, R. Gomperts, R.L. Martin, D.J. Fox, J.S. Binkley, D.J. Defrees, J. Baker, J.P. Stewart, M. Head-Gordon, C. Gonzalez, J.A. Pople, GAUSSIAN 94, Revision C.3, Gaussian, Inc.; Pittsburgh, PA, 1995.

[23] (a) R. Hoffmann, J. Chem Phys. 39 (1963) 1397. (b) K. Tatsumi, A. Nakamura, J. Am. Chem. Soc. 109 (1987) 3195. (c) R. Hoffmann, Angew. Chem. Int. Ed. Engl. 21 (1982) 711.

[24] J.H. Ammeter, H.-B. Bürgi, J.C. Thibeault, R. Hoffmann, J. Am. Chem. Soc. 100 (1978) 3686.

[25] C. Mealli, D.M. Proserpio, CACAO, Universitá di Firenze, Italy, 1992.

[26] S.J. Cyvin, J.E. Rauch, J.C. Decius, J. Chem. Phys. 43 (1965) 4083.

[27] G.M. Scheldrick, in: G.M. Scheldrick, C. Kruger, R. Goddard (Eds.), Crystallographic Computing 3, Oxford University Press, Oxford, 1985, pp. 175–189.

[28] G.M. Scheldrick, SHELX93, Crystallographic Calculation Program, University of Cambridge, 1993.

[29] C.K. Johnson, ORTEP-II, Report ORNL-5138, Oak Ridge National Laboratory, Park Ridge, TN, 1976.

[30] International Tables for X-Ray Crystallography, vol. IV, Kynoch Press, Birmingham, 1974.